Evolution of Spherical Assemblies to Fibrous Networked Pd(II) Metallogels from a Pyridine-Based Tripodal Ligand and Their Catalytic Property

Yong-Ru Liu,[†] Lisi He,[†] Jianyong Zhang,*[,†] Xiaobing Wang,[†] and Cheng-Yong Su*[,†,‡]

MOE Laboratory of Bioinorganic and Synthetic Chemistry, State Key Laboratory of Optoelectronic Materials and Technologies, School of Chemistry and Chemical Engineering, Sun Yat-Sen University, Guangzhou 510275, China, and State Key Laboratory of Organometallic Chemistry, Shanghai Institute of Organic Chemistry, Chinese Academy of Sciences, Shanghai 200032, China

Received October 19, 2008. Revised Manuscript Received December 10, 2008

A series of metal−organic gels (MOGs) were formed in $CH_3OH-CHCl_3$ solution based on L1 and $Pd(COD)(NO_3)_2$ (L1 = 4,4′,4″-(1,3,5-triazine-2,4,6-triyl)tris(*N*-(pyridin-3-ylmethyl)benzamide, COD = cycloocta-1,5-diene) at different ratios. FT-IR, NMR, and fluorescence spectroscopy show that hydrogen bonding, $\pi-\pi$ interaction, and coordination bonding are involved in the gel formation. The morphologies of these metallogels are Pd/L1 ratio dependent ranging from spheres to fibers. The fibrous networked gel shows higher catalytic activity in Suzuki−Miyaura coupling reaction than the spherical gel, acting as recyclable Pd(II) catalyst supported by the air-stable networked gel/xerogel.

Introduction

Studies on supramolecular gels have attracted chemists' attention in recent years because of the numerous potential applications, such as sensors, actuators, molecular devices, catalysts, and so forth.[1] Recently, reports on metallogels are increasing due to their prospective functions in template synthesis, catalysis, and stimuli responsive materials, by the presence of metal centers.[2] Although many organic ligands have been synthesized to build a large number of coordination polymers, in which large sized ligands are especially useful in building metal−organic frameworks (MOFs),[3] there are only a few examples that gels were obtained through coordinative binding between multipodal ligands and metal ions.[4] Because the term MOFs has already been well understood to imply extended metal−ligand compounds that display "long range ordered" one-, two-, or three-dimensional (1D, 2D, or 3D) structures, it might be intelligible to specify the term "metal−organic gels" (MOGs) to describe the metallogels that rely on metal−ligand coordination extending into "short range ordered" 1D, 2D, or 3D structures either via coordination or other supramolecular interactions. An obvious difference between MOFs and MOGs is that the former displays infinite long ranged order with periodic arrangement of asymmetric units while the latter is only characteristic of finite short ranged order with periodically disordered arrangement of the building units. However, presence of comparable structural features between them makes it convenient to speculate the building unit connectivity and assembly process of MOGs, taking advantage of vast crystallographic information readily available for analogous MOFs. Considering the abundance of a great variety of organic ligands and metal ions, studies on MOGs are waiting for extensive exploration.

Low-molecular-weight gelators (LMWGs) can form thermoreversible gels at very low concentrations (ca. 10^{-3} mol/L, typically lower than 2% w/w) in water or organic solvents.[5] Furthermore, LMWGs are known to be able to self-assemble into complex 3D networks through noncovalent interactions such as hydrogen-bonding, $\pi-\pi$ stacking, and van der Waals and hydrophobic interactions.[6] Various metallogelators have also been found to gelate water or organic solvents to form MOGs through the coordination interactions between metal ions and organic ligands, as well

* To whom correspondence should be addressed. E-mail: cesscy@mail.sysu.edu.cn.
† Sun Yat-Sen University.
‡ Shanghai Institute of Organic Chemistry.

(1) (a) Terech, P.; Weiss, R. G. *Chem. Rev.* **1997**, *97*, 3133–3159. (b) Estroff, L. A.; Hamilton, A. D. *Chem. Rev.* **2004**, *104*, 1201–1217. (c) van Esch, J. H.; Feringa, B. L. *Angew. Chem., Int. Ed.* **2000**, *39*, 2263–2266. (d) Sangeetha, N. M.; Maitra, U. *Chem. Soc. Rev.* **2005**, *34*, 821–836. (e) de Loos, M.; Feringa, B. L.; van Esch, J. H. *Eur. J. Org. Chem.* **2005**, 3615–3631. (f) Ajayaghosh, A.; Praveen, V. K.; Vijayakumar, C. *Chem. Soc. Rev.* **2008**, *37*, 109–122.

(2) (a) Kawano, S.-i.; Fujita, N.; Shinkai, S. *J. Am. Chem. Soc.* **2004**, *126*, 8592–8593. (b) Beck, J. B.; Rowan, S. J. *J. Am. Chem. Soc.* **2003**, *125*, 13922–13923. (c) Kishimura, A.; Yamashita, T.; Aida, T. *J. Am. Chem. Soc.* **2005**, *127*, 179–183. (d) Roubeau, O.; Colin, A.; Schmitt, V.; Clerac, R. *Angew. Chem., Int. Ed.* **2004**, *43*, 3283–3286. (e) Kuroiwa, K.; Shibata, T.; Takada, A.; Nemoto, N.; Kimizuka, N. *J. Am. Chem. Soc.* **2004**, *126*, 2016–2021. (f) Miravet, J. F.; Escuder, B. *Chem. Commun.* **2005**, 5796–5798. (g) Yin, J.; Yang, G.; Wang, H.; Chen, Y. *Chem. Commun.* **2007**, 4614–1616.

(3) See for examples: (a) Janiak, C. *Dalton Trans.* **2003**, 2781–2801. (b) Hagrman, P. J.; Hagrman, D.; Zubieta, J. *Angew. Chem., Int. Ed.* **1999**, *38*, 2638–2684. (c) Moulton, B.; Zaworotko, M. J. *Chem. Rev.* **2001**, *101*, 1629–1658. (d) Sun, D.; Ke, Y.; Mattox, T. M.; Parkin, S.; Zhou, H.-C. *Inorg. Chem.* **2006**, *45*, 7566–7568. (e) Rowsell, J. L. C.; Yaghi, O. M. *Microporous Mesoporous Mater.* **2004**, *73*, 3–14. (f) Zheng, S.-R.; Yang, Q.-Y.; Liu, Y.-R.; Zhang, J.-Y.; Tong, Y.-X.; Zhao, C.-Y.; Su, C.-Y. *Chem. Commun.* **2008**, 356–358.

(4) (a) Zhang, J.; Xu, X.; James, S. L. *Chem. Commun.* **2006**, 4218–4220. (b) Wei, Q.; James, S. L. *Chem. Commun.* **2005**, 1555–1556. (c) Yamada, Y. M. A.; Maeda, Y.; Uozumi, Y. *Org. Lett.* **2006**, *8*, 4259–4262.

(5) Llusar, M.; Sanchez, C. *Chem. Mater.* **2008**, *20*, 782–820.

(6) Rieth, S.; Baddeley, C.; Badjic, J. D. *Soft Matter* **2007**, *3*, 137–154.

10.1021/cm802841r CCC: $40.75
Published on Web 01/09/2009

Scheme 1. Molecular Structures of L1 and L2

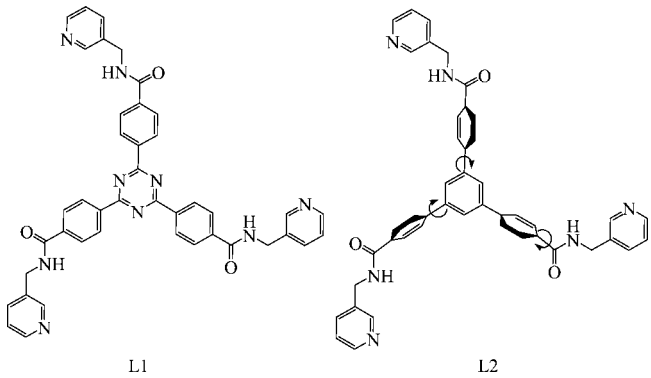

L1 L2

as other supramolecular weak interactions.[7] As a result of the complexity of intermolecular interactions, it is still a challenge to understand how organic ligands and metal ions aggregate into multidimensional MOGs through different interactions. This is probably the key obstacle for building the MOGs from multidentate ligands and metal ions.

In an effort to explore the potential approach to tailor the organic ligand to facilitate formation of MOGs by using noncovalent supramolecular interactions, we prepared a large semirigid tripodal ligand, 4,4″,4″-(1,3,5-triazine-2,4,6-triyl)-tris(*N*-(pyridin-3-ylmethyl)benzamide (L1, Scheme 1), which was chosen and subjected to gelation studies on the basis of following considerations: (a) The amide can serve as hydrogen-bonding donor and acceptor to offer versatile hydrogen-bonding modes, taking account that hydrogen-bonding is often the driving force to gelation in amides/ureas.[8] (b) A large triazine-based plane can serve as a potential $\pi-\pi$ stacking center. The $\pi-\pi$ stacking is usually an important intermolecular interaction in metal complexes containing aromatic nitrogen heterocycles,[9] and existence of various types of $\pi-\pi$ stacking interactions (triazine−triazine, triazine−arene, triazine−pyridine) have been observed for triazine derivatives.[10] (c) The three free-rotating pyridyl pendants connected via methylene groups can fit coordinative geometry of metal ions adaptively. As another consideration, metallogels built on multidentate ligands could be readily disrupted with addition of coordinating reagent or anion.[4a,11] Therefore, the less coordinative nitrate anion rather than acetate[12] was used as counteranion, which could contribute to the gel formation. Since Pd(II)−pyridyl gels are of interest because of their application in catalysis, for example, they have been shown to catalyze the oxidation of benzyl alcohol to benzaldehyde,[2f,12] we report herein the formation of a series of metal−ligand-ratio-dependent MOGs based on Pd(II) and L1. Their catalytic property in Suzuki−Miyaura coupling has also been investigated.

(7) Fages, F. *Angew. Chem., Int. Ed.* **2006**, *45*, 1680–1682.
(8) (a) Piepenbrock, M.-O. M.; Lloyd, G. O.; Clarke, N.; Steed, J. W. *Chem. Commun.* **2008**, 2644–2646. (b) Kim, T. H.; Seo, J.; Lee, S. J.; Lee, S. S.; Kim, J.; Jung, J. H. *Chem. Mater.* **2007**, *19*, 5815–5817.
(9) Janiak, C. *J. Chem. Soc., Dalton Trans.* **2000**, 3885–3896.
(10) Mooibroek, T. J.; Gamez, P. *Inorg. Chem. Acta* **2007**, *360*, 381–404.
(11) Hui, J. K.-H.; Yu, Z.; MacLachlan, M. J. *Angew. Chem., Int. Ed.* **2007**, *46*, 7980–7983.
(12) Xing, B.; Choi, M.-F.; Xu, B. *Chem. Eur. J.* **2002**, *8*, 5028–5032.

Table 1. Gelation Test in Different Solvents

entry	solvent 1[a]	solvent 2[b]	phase[c]
1	MeOH−$CHCl_3$	MeOH	G
2		EtOH	P
3		CH_3CN	G
4	*n*-BuOH−$CHCl_3$	MeOH	G
5		EtOH	P
6		CH_3CN	G
7	DMSO	MeOH	G
8		EtOH	P
9		CH_3CN	G

[a] 0.04 mmol of L1 + 1 mL of corresponding solvent. [b] 0.03 mmol of $Pd(COD)Cl_2$ + 0.06 mmol of $AgNO_3$ + 1 mL of corresponding solvent. [c] G: gel formed at RT; P: precipitate.

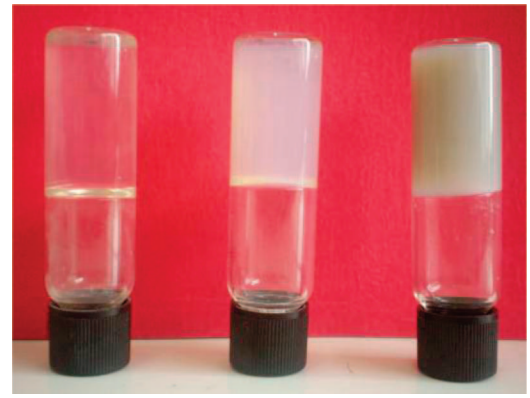

Figure 1. Representative photographic images of the ratio-dependent MOGs, Pd/L, 1:4 (left); 1:2 (middle); 1:1 (right).

Results and Discussion

Gelation Study. The ligand, L1, is soluble in DMF, DMSO, $CHCl_3$-MeOH, and *n*-BuOH-$CHCl_3$ but only slightly soluble in MeOH, EtOH, $CHCl_3$, CH_2Cl_2, THF, acetone, and ethyl acetate. We tested the gelation behavior of L1 and $Pd(COD)(NO_3)_2$. $Pd(COD)(NO_3)_2$ was in situ prepared by reacting $Pd(COD)Cl_2$ and $AgNO_3$ to provide Pd(II) ion in gelation. In situ prepared $Pd(COD)(NO_3)_2$ is chosen since its quantity is more easily controlled than humid-sensitive $Pd(NO_3)_2$. Formation of gels was confirmed in various solvents of DMF, $CHCl_3$-MeOH, and *n*-BuOH−$CHCl_3$ in varying Pd/L1 ratios (for example, Pd/L1 = 3:4, molar ratio, the same below), judged simply by turning the samples upside down (Table 1). It was found that the gel could be formed under a concentration as low as 4.45 mmol/L.

Treating an MeOH solution of $Pd(COD)(NO_3)_2$ (0.02 mol/L) with a MeOH−$CHCl_3$ (v/v 1:1) solution of L1 (0.02 mol/L) gave colorless metallogels in different Pd/L ratios (Figure 1). The time of metallogel forming was shortened along with the increasing of Pd/L ratio ranging from 2 min for the 1:1 gel to 2 h for the 1:4 gel (Table 2). The 1:4 gel is transparent, while the 1:3, 1:2, and 1:1 gels are all turbid, indicating that the particles in the 1:4 gel are more homogenously spread. Heating of either the 1:4 or the 1:1 gel could not transform the gel into solution, when MeOH−$CHCl_3$ was observed to evaporate above the boiling point, showing they are thermally irreversible. When the Pd/L1 ratio was increased up to 3:2, an amorphous precipitate was formed.

The coordinative interactions between Pd(II) and the pyridyl N atoms of L1 were indicated by the changes of ^1H

Table 2. Gelation Ability in Different Pd/L1 Ratios[a]

	ratio Pd/L1							
	4:1	3:1	3:2	1:1	3:4	1:2	1:3	1:4
phase[b]	P	P	P	G	G	G	G	G
gel type				turbid	turbid	turbid	turbid	transparent
time, min				2	5	10	120	120
wt %				1.26	1.32	1.40	1.46	1.50

[a] L1 (0.0267 mol/L) in $CHCl_3-CH_3OH$ (v/v 1:1); $Pd(COD)(NO_3)_2$ (0.02 mol/L) in CH_3OH. [b] G: gel formed at RT; P: precipitate.

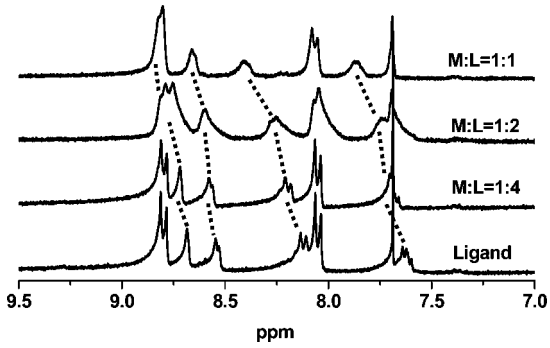

Figure 2. ^1H NMR of L1 and Pd/L1 in $CDCl_3-CD_3OD$ with different Pd/L1 ratios.

NMR signals. Figure 2 shows ^1H NMR spectra of L1 and Pd/L1 of different molar ratios measured in a $CD_3OD-CDCl_3$ mixed solvent. Upon addition of Pd(II) salt, the proton signals on the pyridine ring were shifted downfield. This clearly indicates coordination between the pyridine N donor and Pd(II) ion, which will impart the electron-withdrawing inductive effect on the proximate protons. By contrast, the proton signals on the phenyl rings remained almost unaffected, apparently due to remoteness from the Pd(II) ions. Increasing the M/L ratio led to further downfield shift of the pyridine proton signals, suggesting formation of more Pd−N coordination interactions. However, no signals of "free" ligand were observed even in the Pd:L = 1:4 ratio, which implies that the rapid chemical exchange occurs in this solvent system. In addition, the ^1H NMR signals of the methylene, pyridine rings, and phenyl rings of L1 became broadened upon addition of Pd(II) ion, indicative of oligomerization or polymerization due to coordinative interactions between Pd(II) ions and L1 ligands. Furthermore, the undeuterated solvent protons of CD_3OD and $CDCl_3$ also moved to low field, implying occurrence of the hydrogen bonding interactions between L1 or/and the solvents.

FT-IR spectra for gels and xerogels show similar bands profile comparable to the free ligand L1 (Figures S1 and S2, Supporting Information). The very broad bands at ca. 3300−3400 cm^{-1}, characteristic of hydrogen bonding, were observed for both the ligand and the gels, suggesting that the hydrogen bonding presents in the gels and xerogels like in the ligand. However, this band became broader and stronger along increasing of the Pd/L1 ratio, indicating formation of a larger amount of hydrogen bonding interactions after more complete polymerization upon gelation. The stretching vibration at 1644 cm^{-1} is due to the amide C═O band, and strong bands at 1575−1515 cm^{-1} are assigned to combined N−H deformation and C−N stretching vibrations. The NO_3^- band at approximately 1380 cm^{-1} could not be identified due to overlapping with the ligand except in the spectrum of 1:1 xerogel.

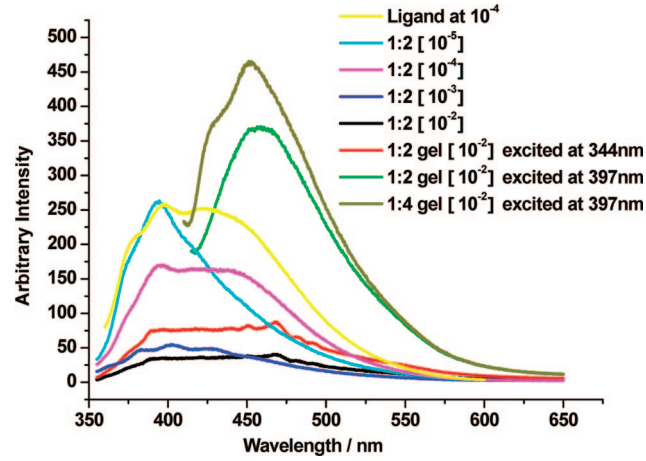

Figure 3. Photoluminescent spectra of the Pd/L = 1:2 and 1:4 systems in gel and solution states at room temperature (excited at 344 nm for all solution states).

Another important factor assisting the formation of such supramolecular gels may be $\pi-\pi$ stacking between aromatic rings of gelators.[13] The triazine rings are apt to form $\pi-\pi$ stacking than benzene rings, and a typical stacking fashion of triazine rings is that the negatively charged nitrogen atoms are aligned with the positively charged carbon atoms between the neighboring rings.[14] For a comparison, we synthesized a structurally similar benzene-centered semirigid tripodal ligand, 1,3,5-tris(*N*-(pyridin-3-ylmethyl)benzamide)benzene (L2, Scheme 1). The ligand L2 prefers the conformation that the outer benzene rings twist apart from the central benzene ring, different from L1 that the triazine rings, and the benzene rings tends to be coplanar. The gelation experiments were carried out under similar conditions, and it was found that no gels but precipitates were formed in various M/L ratios for L2. This result hints that $\pi-\pi$ stacking plays an important role in the gel formation.

Fluorescence spectroscopy may provide important information on the supramolecular organization including $\pi-\pi$ stacked aggregates. The emission spectra of the free ligand L1 and the Pd/L = 1:2 system in different states (solution or gel) at room temperature are shown in Figure 3. The free ligand L1 displays a broad emission profile at the concentration of 10^{-4} M, in which two maximum peaks can be identified at about 395 and 430 nm (excited at 373 nm). When L1 was mixed with $Pd(COD)(NO_3)_2$ in various Pd/L1 molar ratios in solution, the fluorescence was generally reduced probably due to the heavy atom effect. The excitation and the emission bands maxima are slightly shifted compared with those of the free ligand L1, indicating coordination interactions between L1 and Pd(II) ions. At low concentration

(13) (a) Naota, T.; Koori, H. *J. Am. Chem. Soc.* **2005**, *127*, 9324–9325. (b) Tu, T.; Assenmacher, W.; Peterlik, H.; Weisbarth, R.; Nieger, M.; Dötz, K. H. *Angew. Chem., Int. Ed.* **2007**, *46*, 6368–6371. (c) Camerel, F.; Ziessel, R.; Donnio, B.; Bourgogne, C.; Guillon, D.; Schmutz, M.; Iacovita, C.; Bucher, J.-P. *Angew. Chem., Int. Ed.* **2007**, *46*, 2659–2662. (d) Lu, W.; Law, Y.-C.; Han, J.; Chui, S. S.-Y.; Ma, D.-L.; Zhu, N.; Che, C.-M. *Chem. Asian J.* **2008**, *3*, 59–69.
(14) Sun, D.; Ma, S.; Ke, Y.; Petersen, T. M.; Zhou, H.-C. *Chem. Commun.* **2005**, 2663–2665.

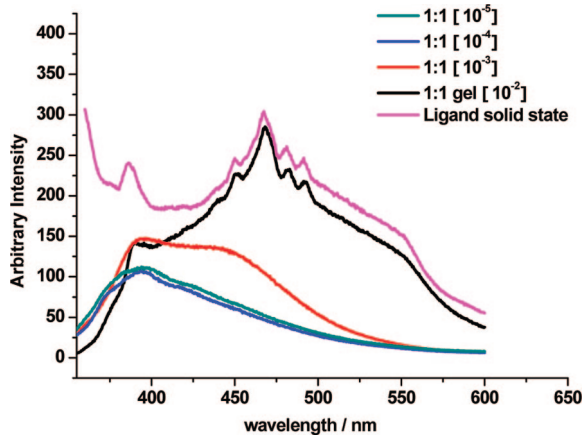

Figure 4. Photoluminescent spectra of the Pd/L = 1:1 system in solution and gel state at room temperature (excited at 344 nm).

(10^{-6} M), the maximum emission appearing at about 395 nm was predominant (excited at 344 nm). When the concentration was increased to 10^{-4} M, the peak at about 440 nm was relatively enhanced. When the concentration was increased to 10^{-2} M, the emissions excited at 344 nm became negligible. After gelation, the emission was enhanced but still remained weak. Alternatively, a strong emission band around 450 nm was sensitized by excitation at 397 nm. This emission may be attributed to the $\pi-\pi$ interaction through the face-to-face *J*-aggregation[15] when the L1 ligands are gelated by Pd(II) ions, indicating presence of $\pi-\pi$ stacked supramolecular aggregation in the gel. The Pd/L1 = 1:4 system exhibits similar fluorescence dependence on the concentration before gelation, while the 1:4 gel shows an intense emission around 450 nm when excited at 397 nm (Figure 3). These results indicate that the $\pi-$-π interactions between the L1 ligands play essential roles in gelation of 1:2 and 1:4 systems.

On the contrary, the emission spectra of the Pd/L1 = 1:1 system display a distinguishable feature as shown in Figure 4. When L1 was treated with $Pd(COD)(NO_3)_2$ at 10^{-5} M in the molar ratio of 1:1, the maximum emission appeared also at about 393 nm (excited at 344 nm), which is comparable with the emission recorded for the 10^{-4} M state. When the concentration was increased to 10^{-3} M, the peak at about 440 nm was also enhanced. These observations are similar to those in Pd/L1 = 1:2 or 1:4 systems. However, it is obvious that the fluorescence of the 1:1 system is increased when concentration is higher than 10^{-4} M, which is in contrast to the remarkable decrease observed in 1:2 and 1:4 systems when concentration is higher than 10^{-4} M. In addition, when gelation occurred at a concentration of 10^{-2} M, a structured fluorescent spectrum was obtained, which is rather similar to the overall profile of the ligand L1 in the solid state (Figure 4). The strongest emission peak appeared at 468 nm with excitation at 344 nm. These results indicate that the gel structure of the 1:1 system is different from the gel structures of 1:2 and 1:4 systems. Appearance of emission at 468 nm suggests that the $\pi-\pi$ stacked aggregation may still be present in the 1:1 gel but is obviously not as significant as in the 1:2 and 1:4 systems.

The above photoluminescent studies show that the luminescence is strongly dependent on the aggregation state due to interactions between ligand L1 and Pd(II) ion, as well as interactions between L1 ligands. In general, formation of gel could lead to enhancement of the fluorescence emission compared to the solution state. On the other hand, the Pd/L = 1:2 or 1:4 systems display much stronger emission than the 1:1 system. These results may support the following speculations: (a) the $\pi-\pi$ interactions are more organized[16] in the gel state than in the solution state, and (b) the gelation in the Pd/L1 = 1:2 and 1:4 systems are predominant by the $\pi-\pi$ stacking over the Pd−N coordination, while (c) the gelation in the Pd/L1 = 1:1 system is more controlled by the Pd−N coordination other than the $\pi-\pi$ stacking. Formation of more Pd−N coordinative interactions in the 1:1 system than in the 1:2 and 1:4 systems have also been confirmed by ^{1}H NMR measurements as discussed before. Gelation may also be influenced by formation of Pd···Pd interactions; however, no MMLCT emission arisen from Pd···Pd interactions could be unambiguously located. In fact, intermolecular d^8-d^8 interaction is less common for mononuclear square planar Pd(II) complexes[17] and may occur only if aided by ligand−ligand $\pi-\pi$ stacking.[13b]

The morphology of xerogels obtained by slow evaporation of the gels with different Pd/L1 ratios in MeOH−$CHCl_3$ was investigated by scanning electron microscopy (SEM). It was found that their morphologies were also strongly dependent on the reaction ratios of $Pd(COD)(NO_3)_2$ and L1 (Figure 5). The as-synthesized Pd/L = 1:4 xerogel consists of spherical particles with an average size of 2 μm (Figure 5a), while a general porous structure with entangled worm-like morphology of 40 nm in diameter is found for the Pd/L = 1:2 xerogel (Figure 5 b,c). With the Pd/L1 ratio increasing from 2:3 to 3:4 to 1:1, a well-defined nanofibrous morphology (Figure 5d,e,f) is gradually formed with a width of about 30−50 nm in diameter. Such an extended network of interlocked fibers is typical of gels.[18] As a comparison, the Pd/L1 = 1.5:1 precipitate has an irregular morphology of sphere/network.

The 1:1 xerogel was also subjected to energy-dispersive X-ray spectroscopy (EDS) analysis, confirming the exclusive composition of C, N, O, and Pd elements (Figure S3, Supporting Information). The X-ray diffraction patterns for the gels and their xerogels show only an amorphous halo (broad "hump"), suggesting random growth when forming gel fibers and spheres during self-assembly. As a representative, the Pd/L = 3:4 xerogel exhibits a N_2-physisorption isotherm of type III,[19] indicative of macroporous solids (Figure 6). The result of adsorption isotherm is consistent with that of SEM microscopy, verifying that the xerogel is generally macroporous with fibrous networks. In addition, the 1:4 gel shows visibly thixotropic behavior. Shaking by

(15) Zhang, G. C.; Liu, M. H. *J. Phys. Chem. B* **2008**, *112*, 7430–7437.
(16) Ryu, S. Y.; Kim, S.; Seo, J.; Kim, Y.-W.; Kwon, O.-H.; Jang, D. J.; Park, S. Y. *Chem. Commun.* **2004**, 70–71.
(17) (a) Akaiwa, M.; Kanbara, T.; Fukumoto, H.; Yamamoto, T. *J. Organomet. Chem.* **2005**, *690*, 4192–4196. (b) Neve, F.; Crispini, A.; Pietro, C. D.; Campagna, S. *Organometallics* **2002**, *21*, 3511–3518.
(18) *Molecular Gels, Materials with Self-Assembled Fibrillar Networks*; Weiss, R. G., Terech, P., Eds.; Kluwer Press: Dordrecht, 2005.
(19) Gregg, S. J.; Sing, K. S. N. *Adsorption, Surface Area and Porosity*, 2nd ed.; Academic Press: New York, 1982.

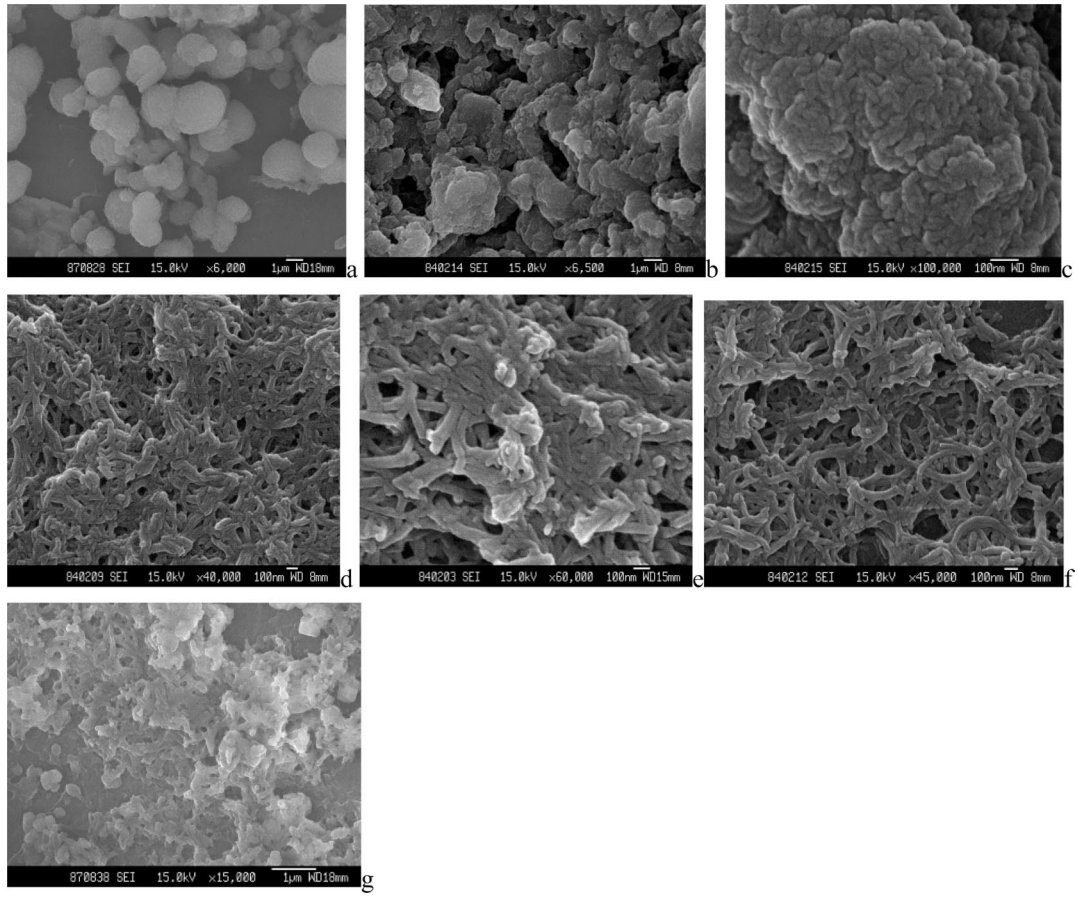

Figure 5. SEM images of xerogels in different Pd/L ratios of (a) 1:4, (b, c) 1:2, (d) 2:3, (e) 3:4, (f) 1:1, and precipitate (g) 1.5:1.

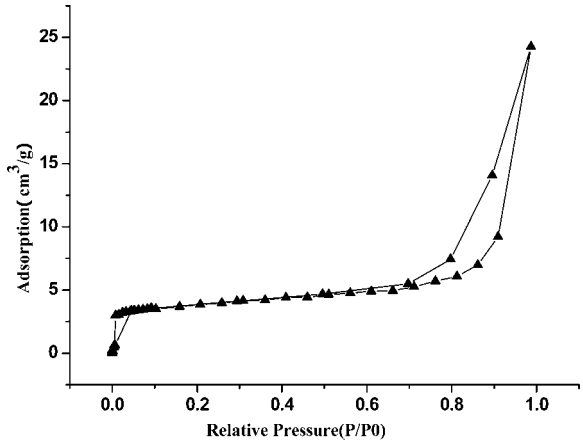

Figure 6. N_2 adsorption−desorption isotherm of the Pd/L = 3:4 xerogel.

Scheme 2. Suzuki−Miyaura Cross-Coupling of 4-Bromopyridine and Phenylboronic Acid

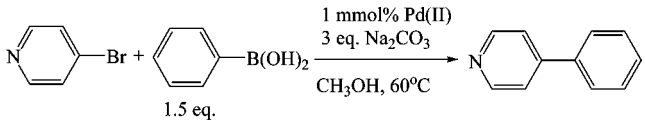

hand for approximately 1 min leads to a free-flowing liquid, which once again gelates on standing for 10 min. In contrast, shaking of the 1:1 gel leads to fragmentation. These behaviors may also suggest that the 1:4 gel has a flexible (individual sphere) structure, while the 1:1 gel has a rigid (3D networked) structure, closely consistent with the SEM results.

Overall, the above results may suggest that the formation of MOGs is subject to different assembly processes due to formation of different PdL_n moieties as depicted in Figure 7. Since the Pd−N coordination is the strongest bonding force, it is reasonable to assume a coordinative building unit which achieves most possible Pd−N bonds to start further assembly. For Pd/L = 1:4 system, PdL_4 moieties could be formed. The gel formation may be mainly attributed to the $\pi-\pi$ stacking among the ligand molecules, as well as hydrogen-bonding interactions between ligand molecules or/and solvents. For the Pd/L = 1:2 gel, formation of a 1D $(PdL_2)_n$ chain which contains half-fully coordinated ligands and half-partially coordinated ligands is possible. Such 1D structure may be extended into 2D or 3D framework via $\pi-\pi$ interactions between the ligands besides hydrogen-bonding. While for the Pd/L = 1:1 gel, the coordination numbers of Pd(II) ions could not be saturated solely by the ligands. Formation of PdL_3 moiety could give rise to two types of 2D coordination networks as shown in Figure 7. The remaining coordination sites of Pd(II) ions may be completed by the NO_3^- anions or amide O atoms from the neighboring 2D network. Therefore, the Pd−N coordination interactions take the priority to direct the gel structure, leaving $\pi-\pi$ interactions and hydrogen-bonding as auxiliary forces to stabilize the gel. Because these interactions do not sustain a long ranged order of the PdL_n moieties, MOGs rather than MOFs are formed, where short ranged order of the PdL_n moieties could exist to give rise to specific morphology depending on metal−ligand ratio.

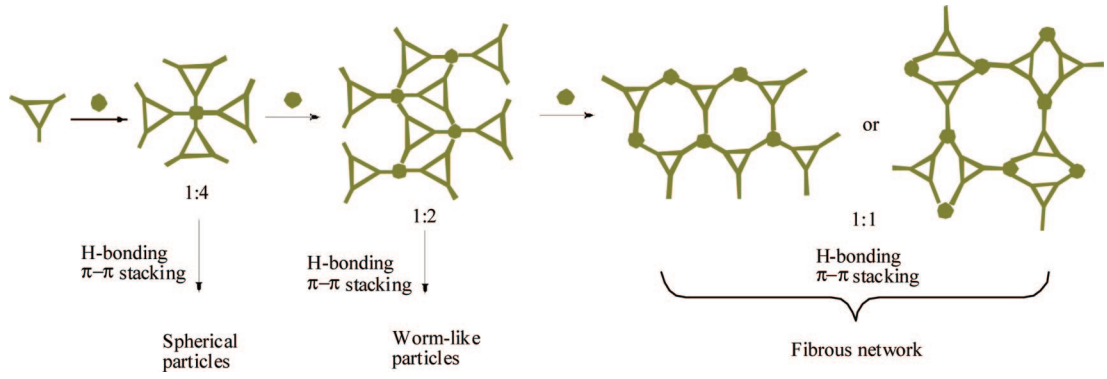

Figure 7. Proposed assembly processes of the short ranged MOFs in different Pd/L1 ratios.

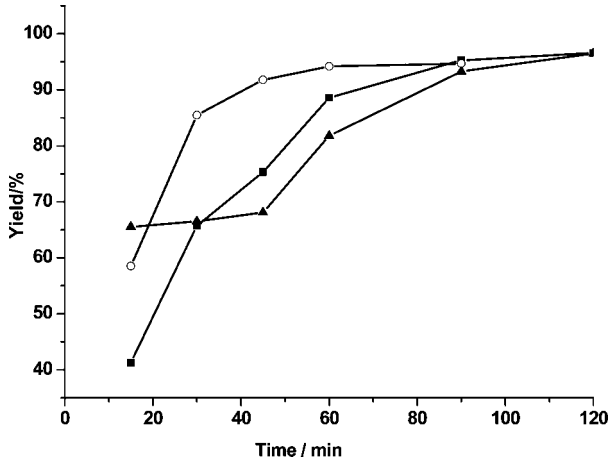

Figure 8. Suzuki−Miyaura coupling of 4-bromopyridine and phenylboronic acid (catalyst: circles, 1:1 gel; triangles, 1:2 gel; squares, 1:4 gel).

Catalytic Activity. Pd(II) complexes are excellent catalyst for many reactions, for example, C−C cross-coupling reaction.[20] Freshly prepared metallogels with different Pd/L1 ratios were subjected to catalytic study in Suzuki−Miyaura coupling. A total of 1 mmol% Pd(II) of the gel was immersed in 8 mL methanol containing 1.0 mmol of 4-bromopyridine, 1.5 mmol of phenylboronic acid, and 3 mmol of Na_2CO_3 at 60 °C under air atmosphere, and the reaction progress was monitored by GC-MS (Scheme 2). The detailed study on the catalytic activities of metallogels with different Pd/L1 ratios showed that the reaction catalyzed by the 1:1 gel took place faster than those catalyzed by the 1:4 and 1:2 gels (Figure 8). Another reaction of iodobenzene and phenylboronic acid also gave the similar results.

We also examined the reaction of various aryl halides with phenylboronic acid catalyzed by the 1:1 gel (Table 3). It was found that the use of iodobenzene or bromoacetophenone (an electron-rich aryl bromide) gave the biaryls in near-quantitative yield, while the reaction of bromobenzene or 4-bromoanisole (an electron-deficient aryl bromide) with phenylboronic acid finished in a short time (15 min), giving a relatively modest yield (28% or 26%).

To examine the activity of the metallogels as recyclable catalysts, the 1:1 gels/xerogels were reused in the reaction of iodobenzene and phenylboronic acid (Table 4). The gels and xerogels are generally stable toward oxygen and water. When catalyzed by the 1:1 gel, iodobenzene reacted with phenylboronic acid to give biphenyl in quantitative yield after 2 h. After the first reaction, the gel could be subjected to a second and third series of the reactions under similar conditions, affording the product in 92 and 30% yields, respectively. When catalyzed by the 1:1 xerogel, iodobenzene reacted with phenylboronic acid to give biphenyl in 92% yield after 2 h. However, after the first reaction, the xerogel could be subjected to a second, third, fourth, and fifth series of the reactions under similar conditions, affording the product in 99, 94, 93, 96, and 95% yields, respectively. It is noteworthy that the 1:1 xerogel maintains its catalytic activity even after at least five uses, showing better recyclable behavior than the 1:1 gel. Xu et al.[12] has reported a gel/xerogel system assembled from Pd(II) ions and a similar tripodal triazine-based ligand. The gel displays better catalysis on the oxidation of benzyl alcohol to benzaldehyde than the xerogel. Our system features an even larger tripodal ligand, and the xerogel shows more effective recyclable

Table 3. Suzuki Coupling of Aryl Halides with Boronic Acids Catalyzed by the Pd/L1 = 1:1 Gel[a]

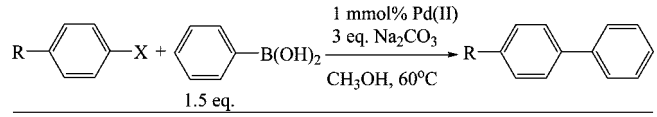

entry	X, R	time, min	yield,[b] %
1	X = I, R = H	90	>99
2	X = Br, R = H	15	28[c]
3	X = Br, R = COMe	15	>99
4	X = Br, R = OMe	15	26[c]

[a] Reaction conditions: 1.0 mmol of aryl halide, 1.5 mmol $PhB(OH)_2$, 1 mmol % of Pd(II) of the catalyst, 3 mmol Na_2CO_3, 8 mL CH_3OH under ambient atmosphere. [b] Determined by GC. [c] Yields reached at 15 min and remained unchanged until 7 h.

Table 4. Effect of Catalytic Runs in Suzuki−Miyaura Coupling Catalyzed by the Gel/Xerogel[a]

entry	run	yield,[b] % (cat.: gel)	yield,[b] % (cat.: xerogel)
1	first	100	92
2	second	92	99
3	third	30	94
4	fourth		93
4	fifth		95

[a] 1.0 mmol iodobenzene, 1.5 mmol phenylboronic acid, 3 mmol Na_2CO_3, 1 mmol% Pd(II) of 1:1 gel/xerogel, 8 mL methanol (60 °C) under ambient atmosphere for 2 h. [b] Determined by GC.

(20) (a) Miyaura, N.; Suzuki, A. *Chem. Rev.* **1995**, *95*, 2457–2483. (b) i Xamena, F. X. L.; Abad, A.; Corma, A.; Garcia, H. *J. Catal.* **2007**, *250*, 294–298.

catalysis than the gel on Suzuki−Miyaura coupling, which was also influenced by the morphology of the gels/xerogels.

Conclusions

In summary, an efficient approach for assembly of metal−organic gels (MOGs) has been accomplished by using $Pd(COD)(NO_3)_2$ and a large semirigid tripodal ligand containing multiply supramolecular interaction sites involving coordination, $\pi-\pi$ interaction, and hydrogen-bonding. The morphology of the gels is found to be largely dependent on the Pd/L1 ratios which result in distinct structural features subject to interplay between Pd−N coordination, $\pi-\pi$ interaction, and hydrogen-bonding. Therefore, simply changing the metal/ligand ratio offers a chance to transform the metallogel morphologies from spheres to fibers, which represents an unprecedented example of gel morphology evolution. On the basis of various spectroscopic results, potential assembly processes of different MOGs have been proposed taking account of the preferential interaction order of the coordinative bonding, $\pi-\pi$ stacking, and hydrogen-bonding, which could be rationally correlated to their gel morphologies, appearance, and thixotropic behaviors. The formation of present metal-to-ligand ratio-dependent gels provides a chance to understand the effect of various supramolecular interactions in the progress of gelation. A unique feature resulting from present Pd/L ratio-dependent gels is that their catalytic activities are different in Suzuki−Miyaura coupling. The fibrous network has been shown to have higher activity than spheres; therefore, such macroporous gel/xerogel network shows potential as a new type of catalytic support.

Experimental Section

All starting materials and solvents were obtained from commercial sources and used without further purification. 2,4,6-Tri-*p*-tolyl-1,3,5-triazine was prepared according to previous literature[21] in the presence of CF_3SO_3H and was subsequently oxidized by CrO_3 to obtain 4,4′,4″-*s*-triazine-2,4,6-triyl-tribenzoic acid.[14] ^{1}H NMR spectra were measured on Mercury-Plus 300 spectrometer. Infrared spectra were measured on a Nicolet Avatrar 330 FT-IR spectrometer with KBr pellets except that those of gels were measured with liquid film on KBr plates.

Synthesis of 4,4′,4″-(1,3,5-triazine-2,4,6-triyl)tris(*N*-(pyridin-3-ylmethyl)benzamide) (L1). 4,4′,4″-*s*-Triazine-2,4,6-triyl-tribenzoic acid (3.30 g, 7.5 mmol) was refluxed together with thionyl chloride (25 mL) for 3 h. Excess thionyl chloride was distilled by heating leaving the 4,4′,4″-(1,3,5-triazine-2,4,6-triyl)tribenzoyl chloride as white solid. THF (25 mL) and Et_3N (4 mL) were mixed with this solid at 0 °C, and pyridin-3-ylmethanamine (2.92 g, 27 mmol) in THF (20 mL) was added dropwise in 1 h. The mixture was stirred overnight at ambient temperature. The white solid obtained was filtered and recrystallized from a mixed solvent of CH_3OH and $CHCl_3$ (v/v 2:1). Yield 3.79 g (71%). ^{1}H NMR (DMSO-d_6, 300 MHz): δ 9.34 (t, 3H), 8.79 (d, 6H), 8.63 (br, 3H), 8.50 (br, 3H), 8.13 (d, 6H), 7.74 (d, 3H), 7.38 (m, 3H), 4.56(d, 6H). IR (cm^{-1}) 3423 (br), 1648 (s), 1517 (vs), 1463 (w), 1406 (w), 1363 (s) 1299 (w), 1018 (w), 827 (w), 713 (w).

Synthesis of Ligand 1,3,5-Tris(*N*-(pyridin-3-ylmethyl)benzamide)benzene (L2). An analogous procedure to L1 was carried out by replacing 4,4′,4″-*s*-triazine-2,4,6-triyl-tribenzoic acid with benzene-1,3,5-tribenzoic acid.[22] ^{1}H NMR (DMSO-d_6, 300 MHz): δ 9.18 (t, 3H), 8.56 (d, 6H), 8.45 (br, 3H), 8.04 (b, 5H), 7.74 (d, 3H), 7.36 (m, 3H), 4.53 (d, 6H).

General Procedure for Preparation of Metallogels. A solution of 0.02 mol/L L1 in $CHCl_3/CH_3OH$ (v/v 1:1) was added to a solution of 0.02 mol/L $Pd(NO_3)_2$ in CH_3OH which was prepared in situ by adding 2 equiv of $AgNO_3$ to $Pd(COD)Cl_2$ in CH_3OH. The resulting reaction mixture was allowed to stand. A colorless gel was formed after minutes or hours.

General Procedure for the Suzuki−Miyaura Cross-Coupling Reaction. In a typical procedure, a mixture of iodobenzene (1.0 mmol), phenylboronic acid (1.5 mmol), Na_2CO_3 (3 mmol), gel/xerogel (0.01 mmol Pd(II)), and 8 mL of MeOH was added to a flask equipped with a stirring bar. The reaction mixture was stirred at 60 °C under ambient atmosphere. After the desired reaction time, a drop of resultant mixture was added to H_2O (ca. 1 mL) and extracted with Et_2O. The organic layer was analyzed by GC-MS and NMR spectroscopy. The gel was packed in a filter bag, while the xerogel was centrifuged for recovering.

SEM-EDX. Field emission scanning electron micrographs were recorded by using a Jeol JSM-6330F instrument after gel samples were slowly evaporated to dryness in air. Prior to examination the xerogels were dried in vacuum and coated with a thin layer of gold. Elemental compositions were determined via semiquantitative energy-dispersive X-ray spectroscopy (EDS) on a Quanta 400F thermal field emission environmental SEM-EDS-EBSD.

Acknowledgment. This work was supported by the NSF for Distinguished Young Scholars of China (Grant 20525310), 973 Program of China (Grant 2007CB815302), and the NSF of China (Grants 20773167, 20731005, J0730420, 20821001).

Supporting Information Available: IR spectra and EDS pattern (PDF). This material is available free of charge via the Internet at http://pubs.acs.org.

CM802841R

(21) Jia, W. L.; Hu, Y. F.; Gao, J.; Wang, S. N. *Dalton Trans.* **2006**, 1721–1728.

(22) Kim, J.; Chen, B. L.; Reineke, T. M.; Li, H. L.; Eddaoudi, M.; Moler, D. B.; O'Keeffe, M.; Yaghi, O. M. *J. Am. Chem. Soc.* **2001**, *123*, 8239–8247.